

# Multi-vortices are Wall Vortices: A Numerical Proof

Stefano BOLOGNESI\* and Sven Bjarke GUDNASON†

*The Niels Bohr Institute, Blegdamsvej 17, DK-2100 Copenhagen Ø, Denmark*

## Abstract

We study the Abrikosov-Nielsen-Olesen multi-vortices. Using a numerical code we are able to solve the vortex equations with winding number up to  $n = 25,000$ . We can thus check the wall vortex conjecture previously made in [1, 2]. The numerical results show a remarkable agreement with the theoretical predictions.

December, 2005

---

\*bolognesi@nbi.dk

†gudnason@nbi.dk

# Contents

<b>1</b>	<b>Introduction</b>	<b>1</b>
<b>2</b>	<b>Theoretical Section</b>	<b>2</b>
2.1	The Wall Vortex Limit . . . . .	3
2.2	The Differential Equations . . . . .	6
2.3	A Non Trivial Check . . . . .	8
<b>3</b>	<b>Numerical Analysis</b>	<b>9</b>
3.1	Quartic Potential and the MIT bag regime . . . . .	10
3.2	Degenerate Vacua and the SLAC bag regime . . . . .	12
3.3	SLAC/MIT phase transition . . . . .	15
<b>4</b>	<b>Conclusion and Further Developments</b>	<b>17</b>

## 1 Introduction

The idea of the wall vortex emerged in [1] when we faced the following situation. Consider a theory that has two degenerate vacua, one in the Higgs phase and another in the Coulomb phase. Then take a domain wall that interpolates between the two vacua and place a monopole on the Coulomb side. What happens if we continuously move the monopole towards the Higgs phase? It is known that a monopole in the Higgs phase cannot exist by itself and must be confined. The only reasonable thing that can happen is that the monopole wall system is continuously transformed into a monopole-vortex-wall. This implies that the confining vortex in the Higgs phase can be continuously transformed into a wall or, in another way, is made of the same stuff as the wall. Thus we call it a wall vortex. Now it is easy to understand what are the forces that keep the vortex soliton together. The wall tension that tends to squeeze the vortex, is nothing but the Derrick [3] collapse force coming from the scalar part

of the action  $\partial\phi\partial\phi + V(\phi)$ . What prevents the soliton from collapsing is a pressure coming from the magnetic flux inside the vortex. The magnetic energy is  $B^2 R^2$ , but we should keep in mind that when varying the radius of the cylinder, what remains constant is not the magnetic field but the flux. In terms of the flux, the magnetic energy is  $\Phi_B/R^2$  and thus a pressure term.

The wall vortex argument, up to this point, was only a qualitative way to understand the continuous transition from a wall to a vortex and also the forces that bind together the soliton. In order to apply this idea also quantitatively we need to find a regime in which the radius of the vortex  $R_V$  becomes much greater than the thickness of the domain wall  $\Delta_W$ . We find that this is exactly the large  $n$  limit where  $n$  is the number of quanta of magnetic fluxes carried by the vortex. It is easy to understand why this happens. The domain wall does not know anything about the magnetic flux and thus its thickness is independent of  $n$ . On the contrary the radius of the vortex depends on  $n$ , in particular it grows as  $n$  grows. This means that the ratio  $\Delta_W/R_V$  can be made arbitrarily small by increasing the parameter  $n$ .

In [2] we applied the wall vortex argument to the general Abelian-Higgs model. In this case there is only one true vacuum, the Higgs vacuum. The Coulomb phase is not a true vacuum of the theory, but due to the symmetry of the problem, it is always a stationary point of the potential. Is it possible, that also in this case, in the large  $n$  limit, the vortex becomes a wall vortex? This was the conjecture made in [2]. The aim of this paper is to prove this conjecture by means of numerical computation.

We organize the paper in the following way. In Section 2 we give a review of the wall vortex idea and we state the theoretical arguments that support the conjecture. Then in Section 3 we present the numerical proof of the conjecture. In Section 3.2 we analyze the original problem when the Coulomb and Higgs phases are degenerate. Finally in Section 4 we conclude with a discussion about the relation between different potentials in the large  $n$  limit.

## 2 Theoretical Section

In this section we provide the theoretical analysis that leads to the wall vortex conjecture. A lot of independent arguments support the wall vortex limit. Part of these arguments are new and part are just a review of [1, 2].

The theory under consideration is the Abelian-Higgs model, which is the relativistic version of the Ginzburg-Landau theory of superconductivity [4]. It is a  $U(1)$  gauge theory coupled to a charged scalar field  $q$

$$\mathcal{L} = -\frac{1}{4e^2}F_{\mu\nu}F^{\mu\nu} - |(\partial_\mu - iA_\mu)q|^2 - V(|q|) . \quad (2.1)$$

The potential  $V(|q|)$  is such that the field  $q$  acquires a vev  $q_0$  and gives mass to the  $U(1)$  photon. In this phase the theory admits vortex solutions called Abrikosov-Nielsen-Olesen (ANO) flux tubes [5, 6]. The ANO vortex is a soliton extended in  $1+1$  dimensions. The usual way is to choose cylindrical coordinates  $(z, r, \theta)$  with the vortex oriented in the  $\hat{z}$  direction. The fields can then be put in the following form

$$\begin{aligned} q &= e^{in\theta}q(r) , \\ A_\theta &= \frac{n}{r}A(r) , \end{aligned} \quad (2.2)$$

where  $q(r)$  and  $A(r)$  are profile functions that must be determined using the equation of motion. The field  $q$  at  $r \rightarrow \infty$  has been chosen to lie in the vacuum manifolds  $|q| = q_0$ . This is necessary to have a finite energy configuration. The solution (2.2) is obtained by choosing the element  $n$  of the homotopy group  $[n] \in \pi_1(\mathbf{S}^1)$ . To have finite energy it is also necessary to turn on a gauge field in order for the covariant derivative  $Dq$  to vanish. This creates a magnetic flux that is exactly proportional to the topological number  $n$ .

## 2.1 The Wall Vortex Limit

Now we describe what is the wall vortex and then we claim that multi-vortices are wall vortices in the large  $n$  limit.

The main idea is that the Coulomb phase  $q = 0$ , even if it is not the true vacuum of the theory, is always a stationary point of the potential. This in fact is a trivial observation but, as we will see, it is full of non-trivial consequences. In general there are two cases described in Figure 1. The Coulomb phase is a false vacuum with energy density  $V(0) = \varepsilon_0$  and can be metastable or instable. We call  $v_0$  the highest peak of the potential between the Coulomb and the Higgs phase.

Now comes the first assumption. Consider the domain wall interpolating between the true and the false vacuum as an independent object with tension and thickness,

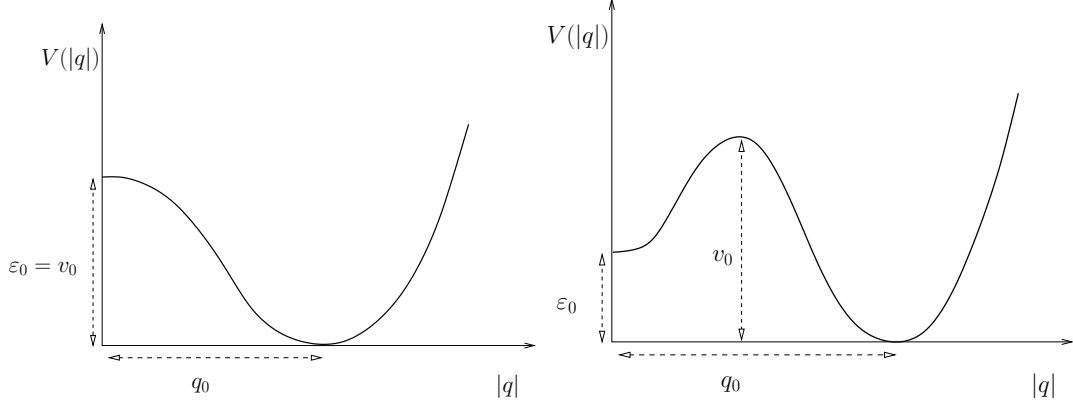


Figure 1: Two possibilities for the Higgs potential. In the first case the Coulomb phase is unstable while in the second case it is metastable.

respectively:

$$T_W \sim \sqrt{v_0} q_0, \quad \Delta_W \sim \frac{q_0}{\sqrt{v_0}}. \quad (2.3)$$

This domain wall does not really exist as an independent object. The energy density  $\varepsilon_0$  gives a negative pressure that tends to eliminate the Coulomb half space leaving only the Higgs vacuum. But, as we will see, it can exist in the vortex solution where the negative pressure is counter balanced by the pressure of the magnetic field. The key point is that the domain wall maintain its “identity” even if we change the quanta of magnetic flux  $n$ . Thus in the large  $n$  limit the radius of the vortex  $R_V$  becomes large while the thickness of the wall  $\Delta_W$  remains fixed. This is the key assumption that needs to be proven.

For the moment let’s assume that the wall has its own identity and then go on to the consequences. The wall vortex is a flux tube obtained in the following way. We compactify the domain wall on a cylinder of radius  $R$ , keeping the Coulomb phase inside and the Higgs phase outside. Then we turn on a magnetic flux inside the cylinder and we write the tension of the tube as function of the radius :

$$T(R) = \frac{2\pi n^2}{e^2 R^2} + T_W 2\pi R + \varepsilon_0 \pi R^2. \quad (2.4)$$

There are three forces that enter the game. Two of them tend to squeeze the tube and are due to the tension of the wall and to the energy density  $\varepsilon_0$ . This is nothing but the Derrick collapse coming from the scalar part of the Lagrangian. The last force is a positive pressure that comes from the magnetic field inside the tube.

There are two regimes in which (2.4) easily can be solved: the SLAC bag and the MIT bag.<sup>1</sup>

**SLAC bag:** This regime is when  $n$  satisfies the two conditions

$$\frac{q_0^2 e}{\sqrt{v_0}} \ll n \ll \frac{q_0^2 e v_0}{\varepsilon_0^{3/2}} . \quad (2.5)$$

The first condition is that the radius  $R_V$  is much bigger than the thickness of the wall  $\Delta_W$ . The second condition is that the surface term  $T_W 2\pi R$  dominates over the volume term  $\varepsilon_0 \pi R^2$ . In this limit

$$T_{\text{SLAC}} = 3\sqrt[3]{2}\pi \left(\frac{T_W}{e}\right)^{2/3} n^{2/3} , \quad R_{\text{SLAC}} = \sqrt[3]{2} \frac{1}{e^{2/3} T_W^{1/3}} n^{2/3} . \quad (2.6)$$

**MIT bag:** This regime is when  $n$  satisfies the condition

$$\frac{q_0^2 e v_0}{\varepsilon_0^{3/2}} \ll n . \quad (2.7)$$

In this limit the volume term in (2.4) dominates over the surface term and

$$T_{\text{MIT}} = 2\sqrt{2}\pi \frac{\sqrt{\varepsilon_0}}{e} n , \quad R_{\text{MIT}} = \sqrt[4]{2} \frac{1}{e^{1/2} \varepsilon_0^{1/4}} \sqrt{n} . \quad (2.8)$$

Note that the tension is proportional to  $n$ , as in the BPS case.

Let's write for clarity the complete story of multi-vortices. At the value  $n \gg \frac{q_0^2 e}{\sqrt{v_0}}$ , where the radius is much bigger than the thickness of the wall, the multi-vortex becomes a wall vortex. If the parameter  $v_0$  is much bigger than  $\varepsilon_0$ , the wall vortex can be subdivided into two different regimes. In the first one  $n \ll \frac{q_0^2 e v_0}{\varepsilon_0^{3/2}}$  and the surface term dominates over the volume term and we call it the SLAC bag regime. In this regime the tension scales like  $n^{2/3}$ . When  $n \sim \frac{q_0^2 e v_0}{\varepsilon_0^{3/2}}$ , the volume term starts to be comparable to the surface term and thus a second order phase transition between the SLAC bag and the MIT bag takes place. Note that the MIT bag regime, whenever  $\varepsilon_0 \neq 0$ , is always present and always dominates in the large  $n$  limit.

Now let's write the conjecture for clarity:

*Consider the Abelian Higgs model (2.1) with a general potential that has a true vacuum at  $|q| = q_0 \neq 0$  and a Coulomb phase with energy density  $V(0) = \varepsilon_0 \neq 0$ .*

---

<sup>1</sup>We have taken the names from the bags models of hadrons: the MIT bag [9] and the SLAC bag [10]. In the Friedberg-Lee model [11] they arise as different limits.

Call  $T_V(n)$  the tension of the vortex with  $n$  units of magnetic flux. The conjecture is that

$$\lim_{n \rightarrow \infty} T_V(n) = T_{\text{MIT}}(n) . \quad (2.9)$$

## 2.2 The Differential Equations

The differential equations for the profile functions of the vortex (2.2) are

$$\begin{aligned} \frac{d^2 q}{dr^2} + \frac{1}{r} \frac{dq}{dr} - n^2 \frac{(1-A)^2}{r^2} q - \frac{1}{2} \frac{\delta V}{\delta q} &= 0 , \\ \frac{d^2 A}{dr^2} - \frac{1}{r} \frac{dA}{dr} + 2e^2(1-A)q^2 &= 0 , \end{aligned} \quad (2.10)$$

where  $n$  is the winding number. We are looking for some limit of the parameters so that the vortex really looks like a wrapped wall. In this limit the profile functions should be:

$$\begin{aligned} q(r) &= q_0 \theta_H(r - R_V) , \\ A(r) &= r^2/R_V^2 \quad 0 \leq r \leq R_V , \\ A(r) &= 1 \quad r \geq R_V , \end{aligned} \quad (2.11)$$

where  $\theta_H$  is the Heaviside step function. Note that the magnetic field is  $\propto A'/r$  and is constant inside the vortex and zero outside.

First of all we manipulate the differential equations (2.10) to simplify them. The potential can be written as a dimensionless function

$$V(q) = \varepsilon_0 \mathcal{V} \left( \frac{q}{q_0} \right) , \quad (2.12)$$

where  $\varepsilon_0$  is the value of the potential at  $q = 0$  and  $q_0$  is the vev at which the potential vanishes. The rescaled potential fullfills  $\mathcal{V}(0) = 1$  and  $\mathcal{V}(1) = 0$ . We also rescale the scalar field  $q = q_0 \chi$ . In the case of a quartic potential the only one with the required properties is  $\mathcal{V}(\chi) = (\chi^2 - 1)^2$ . After these rescalings the equations (2.10) for the profiles become:

$$\frac{d^2 \chi}{dr^2} + \frac{1}{r} \frac{d\chi}{dr} - n^2 \frac{(1-A)^2}{r^2} \chi - a \frac{\delta \mathcal{V}}{\delta \chi} = 0 , \quad (2.13)$$

$$\frac{d^2 A}{dr^2} - \frac{1}{r} \frac{dA}{dr} + b(1-A)\chi^2 = 0 . \quad (2.14)$$

There are three parameters that enter the game:

$$n, \quad a = \frac{1}{2} \frac{\varepsilon_0}{q_0^2}, \quad b = 2e^2 q_0^2. \quad (2.15)$$

Now comes the first non-trivial hint for the wall vortex conjecture. If the wall limit exists, then formula (2.8) can be trusted in this limit. But the radius of the vortex  $R_V$  comes from equations (2.10) and must depend only on the three relevant parameters  $n, a, b$ . In general a function of  $n, e, \varepsilon_0, q_0$  cannot be expressed as a function of  $n, a, b$ , but for (2.8) this is possible:

$$R_{\text{MIT}} = \sqrt[4]{2} \frac{\sqrt{n}}{\sqrt[4]{ab}}. \quad (2.16)$$

If we would not have found such an expression, we would have concluded that the wall vortex limit does not exist. This result encourages us to go on.

In this paragraph we look for a limit in which the radius of the vortex remains constant and the solution approaches the wall vortex (2.11). To do so we need to rescale also the parameters  $a$  and  $b$  such that the radius remains fixed while approaching the large  $n$  limit. The  $\chi$  profile must become a step function: it is zero inside  $R_V$ , it goes from zero to one in a distance  $\Delta_W$ , and then remains constant at one. Thus  $\chi''$  in equation (2.13) develops a  $\delta'(r - R_V)$  singularity or, in terms of  $\Delta_W$ ,  $\chi'' \sim 1/\Delta_W^2$ . To counter balance this divergence in (2.13) we must have that  $a$  goes to infinity like  $1/\Delta_W^2$ . Now consider the second equation (2.14) where  $A''(R_V)$  has a  $(2/R_V)\delta(r - R_V)$  singularity, or in terms of  $\Delta_W$ ,  $A''(R_V) \sim 1/(R_V\Delta_W)$ . Since  $(1 - A)\chi$  is of order  $\Delta_W/R_V$  around  $R_V$ , we must also send  $b$  to infinity like  $1/\Delta_W^2$ . Now we can reformulate the conjecture of the wall limit in another equivalent way.

*Consider the succession of parameters  $a_n = na_1$  and  $b_n = nb_1$  and name the solution of (2.13) and (2.14) with the vortex boundary conditions,  $\chi_{n,a_n,b_n}(r)$  and  $A_{n,a_n,b_n}(r)$ . In the limit  $n \rightarrow \infty$*

$$\lim_{n \rightarrow \infty} \chi_{n,a_n,b_n}(r) \rightarrow \theta_H(r - R_V), \quad (2.17)$$

$$\lim_{n \rightarrow \infty} A_{n,a_n,b_n}(r) \rightarrow \begin{cases} r^2/R_V^2 & 0 \leq r \leq R_V, \\ 1 & r > R_V. \end{cases}$$

This limit has been chosen such that the radius of the vortex remains constant  $R_V = \sqrt[4]{2/(a_1 b_1)}$  and also the ratio  $a_n/b_n$  remains constant. The information about



the ratio  $a/b$  disappears in the wall vortex limit. It is only related to the shape of the limiting functions  $\chi_{n,a_n,b_n}(r)$  and  $A_{n,a_n,b_n}(r)$ . Probably a stronger version of the conjecture is true: the ratio  $a_n/b_n$  is kept limited from above and from below during the limit, so that it does not go neither to infinity nor to zero.

The ratio  $a/b$  has also another important meaning. In fact, in the case of quartic potential, it is essentially the parameter  $\beta$  that measures the ratio between the Higgs and the photon mass:

$$\beta = \frac{m_H}{m_\gamma} = 8 \frac{a}{b} . \quad (2.18)$$

When  $\beta < 1$  the Higgs attraction dominates and the vortices are of Type I. When  $\beta > 1$  the photon repulsion dominates and the vortices are of Type II. When  $\beta = 1$  the vortices are BPS, this means that the tension is a linear function of  $n$  and the distance between different vortices is the vortex moduli space.

## 2.3 A Non Trivial Check

Now we make a non-trivial check of the result (2.8) using the famous example solved by Bogomol'nyi [12]. When the potential is

$$V(|q|) = \frac{e^2}{2} (|\phi|^2 - \xi)^2 , \quad (2.19)$$

the tension is

$$T_{\text{BPS}} = 2\pi n \xi , \quad (2.20)$$

for all  $n$ . Solving the model with our trick, the result must coincide with eq. (2.20). For the BPS potential (2.19), the energy density of the instable Coulomb vacuum is  $\varepsilon_0 = e^2 \xi^2 / 2$ . Using (2.8), we find exactly (2.20). This could hardly be just a coincidence.

It is well known that  $n$  BPS vortices have a moduli space of real dimension  $2n$  where the coordinates can be interpreted as the position of every constituent 1-vortex [13]. In the BPS bag we expect to recover this moduli space and we expect it to have infinite dimension. In fact this space consist of the closed surfaces with fixed area. More details will be discussed in [14] in relation with the multi-monopole moduli space.

### 3 Numerical Analysis

This is the central part of the paper. With the help of numerical computations we are going to prove the conjecture made in the previous section. The strategy is to prove the conjecture as it has been reformulated in (2.17), that is, we rescale the parameters of the theory such that the radius of the vortex remains constant and the thickness of the wall goes to zero.

The code<sup>2</sup> used to solve the system of differential equations (2.13-2.14) uses a numerical method called finite difference method. The boundary conditions are at the singular points of the system 0 and  $\infty$  and thus we use the limits:

$$\begin{aligned} \lim_{r \rightarrow 0} (2A(r) - rA') &= 0, & \lim_{r \rightarrow 0} (n\chi(r) - r\chi') &= 0, \\ \lim_{r \rightarrow \infty} \left( A(r) + \frac{1}{\sqrt{nb}} A' \right) &= 1, & \lim_{r \rightarrow \infty} \left( \chi(r) + \frac{1}{\sqrt{8na}} \chi' \right) &= 1, \end{aligned} \quad (3.1)$$

Other methods often used are e.g. the shooting method, but in case of a step function insanely high accuracy is needed. Still for the finite difference method, the step function poses severe problems and the technique to deal with the problem is to use a combination of a continuation method and feeding the algorithm with an approximate solution. Also the rescaling of the equations such that the radius of the vortex is constant is an important factor for solving the equations. The finite difference method transforms the problem into a matrix equation

$$F_{ij} = 0, \quad i = 1, \dots, \text{meshsize}, \quad j = 1, 2, \quad (3.2)$$

which, when using a continuation method, looks like

$$G_{ij}(t) = 0, \quad t \in [0, 1], \quad (3.3)$$

where the problem is easy to solve when  $t = 0$  and hard to solve for  $t = 1$ . Then the solver will try to increase the hardness in sufficiently small steps until the final problem  $t = 1$  is solved. Whenever a solution has been found it is fed to the solver as an approximate solution which is the solution to the problem for  $t = 0$  and for sufficiently small steps it is then possible to achieve higher winding number  $n$ . The approximate solutions tell the solver where to look for the solution in phase space.

---

<sup>2</sup>The code is written in the mathematical language Maple.

### 3.1 Quartic Potential and the MIT bag regime

The simplest case is the quartic potential. After the rescaling (2.12) there is only one quartic potential to be considered:

$$V(\chi) = (\chi^2 - 1)^2 \quad (3.4)$$

The following figures show the results of the numerical program. Figure 3 is the BPS case where  $\beta = 1$ , Figure 2 is the type I case with  $\beta = 1/16$  and Figure 4 is the type II case with  $\beta = 16$ . In every case we present the profiles for small  $n = 100$  and large  $n$ . At  $n = 25,000$  the step function for  $\chi(r)$  is evident. Note that in the large  $n$  limit the information of  $\beta$  is almost lost and the profiles are all the same. The case  $n = 100$  is interesting because we can see the difference among BPS, type I and type II while approaching the wall vortex limit.

As another check we now evaluate the tension of the vortex. If we directly insert the ansatz (2.2) into the energy density derived from the Lagrangian (2.1), we obtain:

$$T_V(n) = 2\pi \int r dr \left[ \frac{1}{2e^2} \left( \frac{nA'}{r} \right)^2 + \frac{n^2}{r^2} (1 - A)^2 q^2 + q'^2 + V(q) \right]. \quad (3.5)$$

Now we want to verify the conjecture in its first formulation (2.9), that is by increasing  $n$  without changing the parameters of the theory. We introduce a new quantity  $\mathcal{T}(n)$  defined to be the ratio between the real tension and the BPS tension:

$$\mathcal{T}(n) = \frac{T_V(n)}{T_{\text{BPS}}(n)} \quad (3.6)$$

For this new quantity the conjecture (2.9) is simply  $\lim_{n \rightarrow \infty} \mathcal{T}(n) = 1$ .

Figure 5 shows the three plots of  $\mathcal{T}(n)$  for  $\beta = 1/16, 1, 16$ , respectively. The quantity  $\mathcal{T}(n)$  has also an important physical meaning: it is the tension per unit of flux carried by the vortex. This means that from the sign of the derivative  $d\mathcal{T}/dn$ , we can read if there is attraction or repulsion between vortices. Figure 5 is consistent with the ordinary expectation of type I and type II superconducting vortices. If we take for example  $\beta = 1/16$  (type I vortices) the derivative  $d\mathcal{T}/dn$  is negative and this means that there is attraction. For  $\beta = 16$  the function  $\mathcal{T}$  grows up to 1 and this means that there is repulsion (type II vortices). Our theory predicts also the way  $\mathcal{T}(n)$  approaches 1 at infinity. The radius of the vortex in the large  $n$  limit is  $R_{\text{MIT}} \sim \sqrt{n}$  while the thickness of the wall  $\Delta_W$  remains constant. This mean that the deviation from the “perfect” wall vortex is of order  $1/\sqrt{n}$ . In Figure 5 we show also the fits  $\mathcal{T}(n) \sim 1 + \text{const}/\sqrt{n}$  and they perfectly agree with the numerical data.

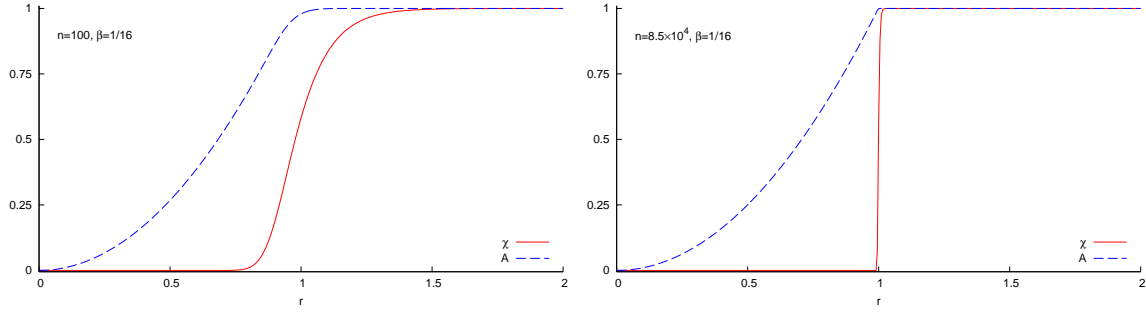


Figure 2:  $\chi(r)$  and  $A(r)$  profiles for  $\beta = 1/16$  and  $n = 100, n = 85,000$ .

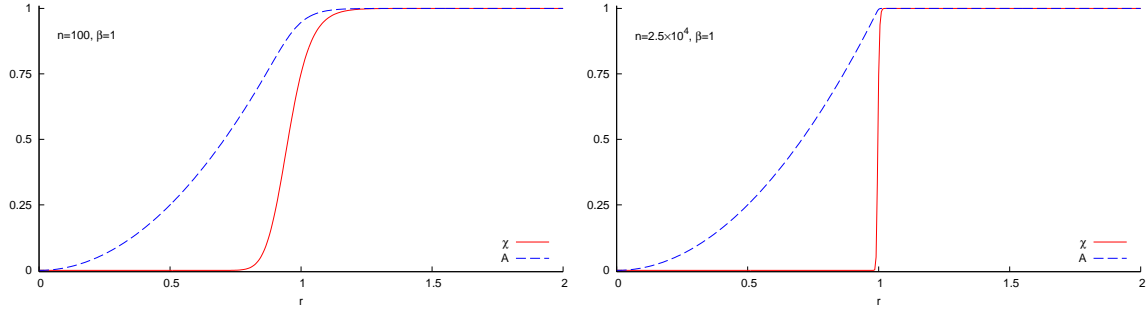


Figure 3:  $\chi(r)$  and  $A(r)$  profiles for  $\beta = 1$  and  $n = 100, n = 25,000$ .

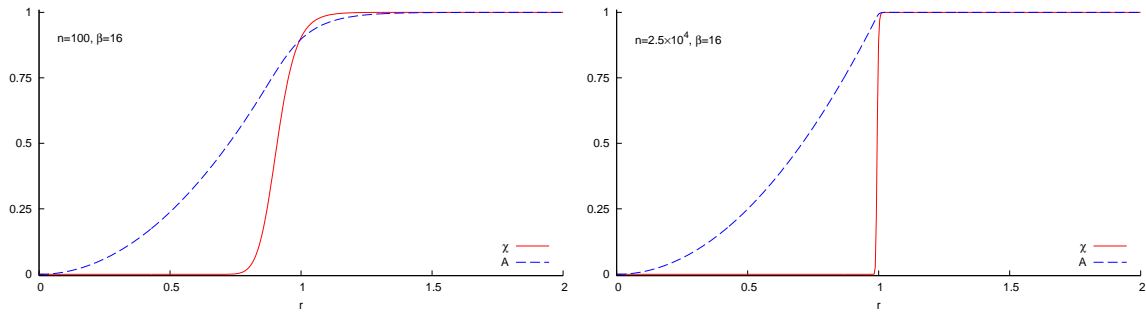


Figure 4:  $\chi(r)$  and  $A(r)$  profiles for  $\beta = 16$  and  $n = 100, n = 25,000$ .

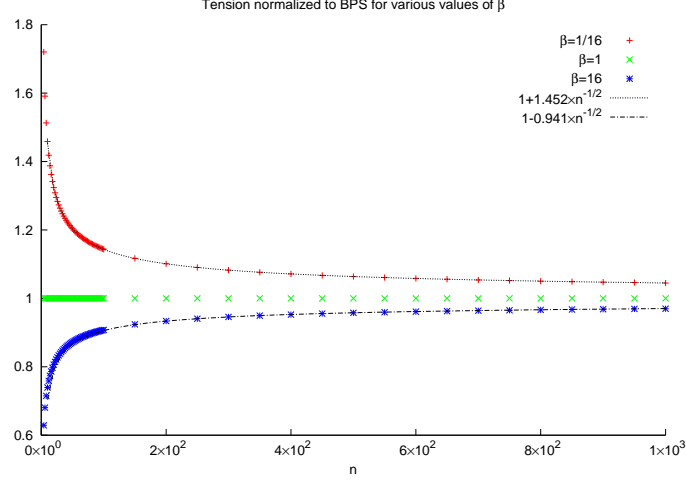


Figure 5: Plot of the normalized tension  $\mathcal{T}$  as function of  $n$  for the three cases  $\beta = 1/16, 1, 16$ .

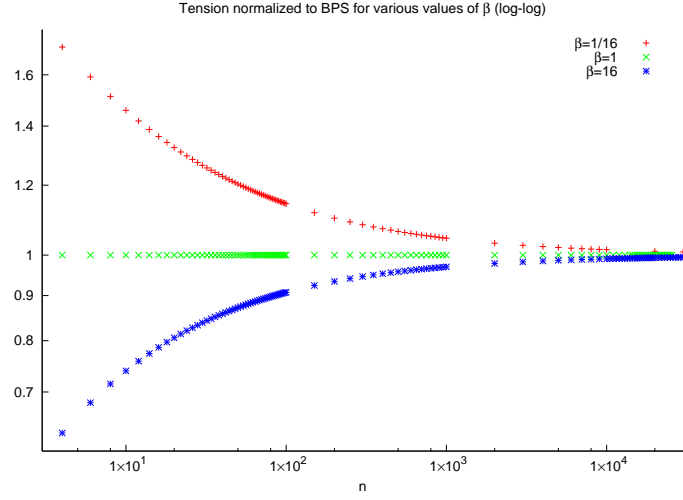


Figure 6: Plot of the normalized tension  $\mathcal{T}$  in the log-log graph.

### 3.2 Degenerate Vacua and the SLAC bag regime

Now we consider the case of degenerate vacua when the potential is like that of Figure 7. Since the Coulomb vacuum energy density vanishes, there is no MIT regime in the large  $n$  limit. The conjecture (2.9) must then be replaced by

$$\lim_{n \rightarrow \infty} T_V(n) = T_{\text{SLAC}}(n) . \quad (3.7)$$

If we want to test the conjecture with our numerical code, it is necessary to find

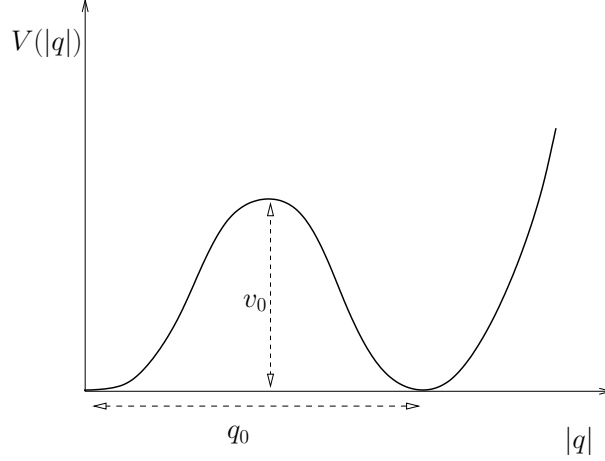


Figure 7: The Coulomb phase and the Higgs phase are the two degenerate vacua of the potential.

a rescaling of the parameters so that the radius of the vortex remains fixed while the thickness of the wall converges to zero. Since the large  $n$  limit is a SLAC bag regime, we must properly modify all the analysis that we have done in subsection 2.2. This has already been done in [1] so we present only a brief description. The equation (2.12) must now be substituted with

$$V(q) = v_0 \mathbf{V}\left(\frac{q}{q_0}\right) . \quad (3.8)$$

The differential equations (2.13-2.14) are the same and the three relevant parameters are

$$n , \quad a = \frac{1}{2} \frac{v_0}{q_0^2} , \quad b = 2e^2 q_0^2 . \quad (3.9)$$

The radius of the SLAC bag (2.6) can be rewritten in terms of the three relevant parameters

$$R_{\text{SLAC}} \sim \frac{n^{2/3}}{a^{1/6} b^{1/3}} . \quad (3.10)$$

We can now give the new formulation of the conjecture.

*Consider the succession of parameters  $a_n = n^{4/3} a_1$  and  $b_n = n^{4/3} b_1$  and call the solution of (2.13) and (2.14) with the vortex boundary conditions,  $\chi_{n,a_n,b_n}(r)$  and*

$A_{n,a_n,b_n}(r)$ . In the limit  $n \rightarrow \infty$

$$\lim_{n \rightarrow \infty} \chi_{n,a_n,b_n}(r) \rightarrow \theta_H(r - R_V) , \quad (3.11)$$

$$\lim_{n \rightarrow \infty} A_{n,a_n,b_n}(r) \rightarrow \begin{cases} r^2/R_V^2 & 0 \leq r \leq R_V , \\ 1 & r > R_V . \end{cases}$$

This limit has been chosen so that the radius of the vortex remains constant  $R_V \sim n^{2/3} a_n^{-1/3} b_n^{-1/6} = a_1^{-1/3} b_1^{-1/6}$  and also the ratio  $a_n/b_n$  remains constant. The ratio  $a/b$  disappears in the wall limit and is only related to the shape of the limiting functions  $\chi_{n,a_n,b_n}(r)$  and  $A_{n,a_n,b_n}(r)$ .

For the computation we take the simplest potential with the Coulomb and Higgs degenerate vacua:

$$V(\chi) = \chi^2(\chi^2 - 1)^2 . \quad (3.12)$$

In Figure 8 we have plotted the tension per unit of flux  $T(n)/n$  for three different values of  $a/b$ . As predicted by the theory all the lines converge to  $T/n \propto n^{-1/3}$  as  $n$  becomes large.

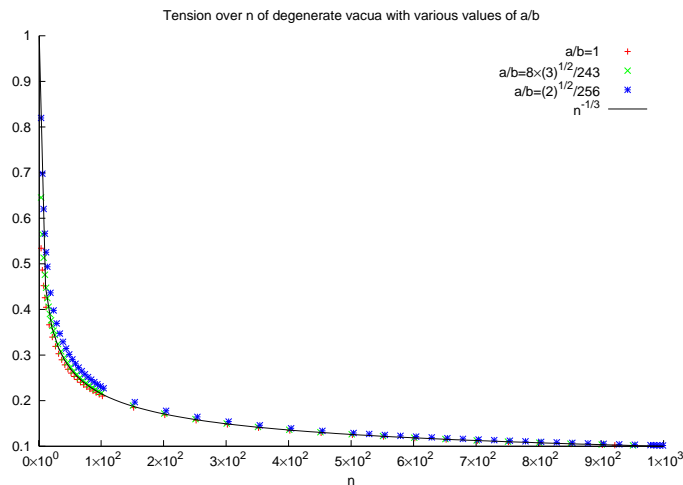


Figure 8: Tension per unit of flux for three different values of  $a/b$ . At large  $n$ ,  $\mathcal{T} \propto n^{-1/3}$  as predicted by the theory.

In Figure 9 we have instead plotted  $T(n)/n^{2/3}$ . In this way is more easy to see the SLAC regime since at infinity all the three lines approaches a constant. In this plot we can also see the first order deviation from the “perfect” SLAC bag. Since the

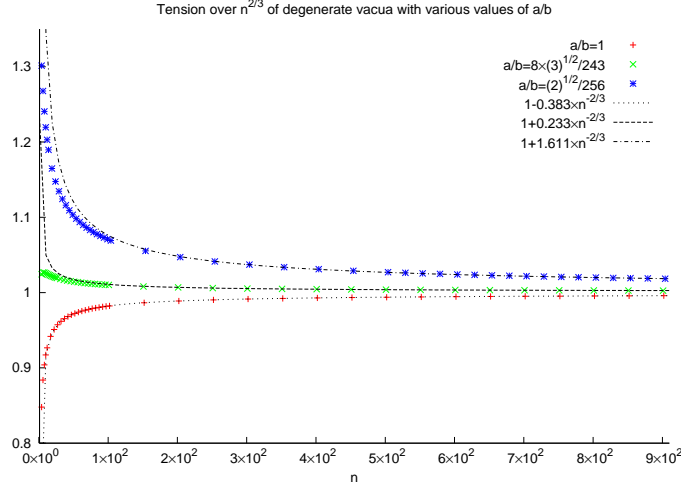


Figure 9: Tension divided by  $n^{2/3}$  for three different values of  $a/b$ . At large  $n$  they approach a constant with an error of order  $1/n^{2/3}$ .

radius  $R_{\text{SLAC}} \propto n^{2/3}$  while the thickness of the wall remains constant, we expect a deviation of order  $1/n^{2/3}$ . The plots with corresponding fits confirm this expectation.

An interesting question is if there exists a kind of BPS notion also for the degenerate vacua potential. Maybe there do exist some potential and some particular value of  $a/b$  for which the tension not only approaches  $T_{\text{SLAC}}$  as  $n$  goes to infinity but is exactly equal to it for all values of  $n$ .

### 3.3 SLAC/MIT phase transition

Another thing to be checked is the presence of a window, namely the SLAC regime, when the Coulomb vacuum is metastable and the peak  $v_0$  is much greater than the energy density  $\varepsilon_0$ . To obtain this regime we need a potential like the second of Figure 1 with  $v_0 \gg \varepsilon_0$ . The theoretical analysis predicts that in the windows of parameters (2.5) the tension and the radius scale like eq. (2.6).

The simplest way to obtain such a potential is to add an opportune  $\chi^6$  interaction:

$$V(\chi) = (\sigma\chi^2 + 1)(\chi^2 - 1)^2 \quad (3.13)$$

The conditions  $V(0) = 1$  and  $V(1) = 0$  leave one free parameter  $\sigma$  that essentially measures the height of the peak of the potential. When  $\sigma$  is great enough the peak



is at  $\chi = 1/\sqrt{3}$  and has the value  $v_0 = 4\sigma/27$ .

We need quite a big  $\sigma$  to detect the window (2.5). In Figure 10 we have plotted the profile  $\chi(r)$  for  $\sigma = 500$ . For this computation we have used the rescaling  $a_n = na_1$ ,  $b_n = nb_1$ . In this rescaling the large  $n$  limit should be a step function with constant radius  $R_{\text{MIT}} = 1$ . What we should see, to confirm the theory, is that the  $\chi(r)$  profile becomes a step function much before reaching the MIT regime. The radius of the wall vortex should be governed by the SLAC law and should increase as  $n^{1/3}$ . When the radius reaches 1 there should be a phase transition between the SLAC regime and the MIT regime where the radius remains constant as 1.

Using the rescaling  $a_n = na_1$ ,  $b_n = nb_1$  the numerical computation cannot reach high enough  $n$  to reach the phase transition. Nevertheless it is possible to detect the presence of the SLAC regime just by looking at Figure 10. The profile  $\chi(r)$  becomes a step function at a radius much lower than 1 and then the radius increases towards 1.

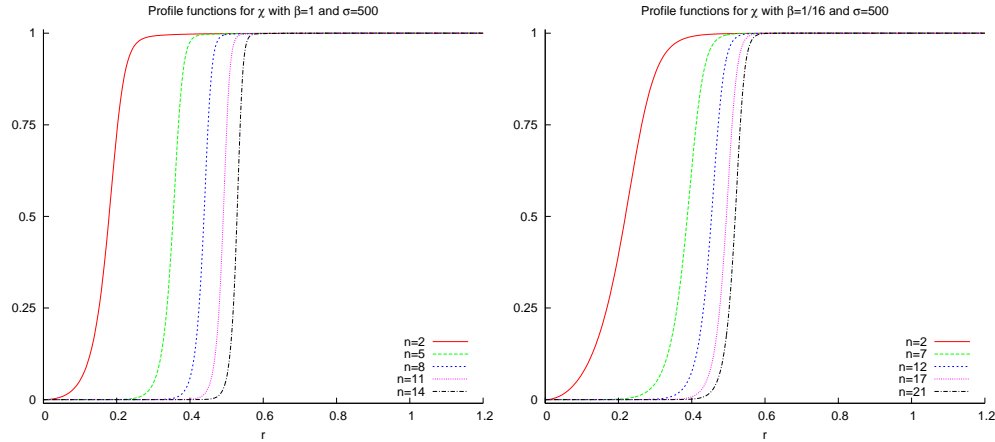


Figure 10: Profile  $\chi(r)$  for the potential (3.13) with  $\sigma = 500$ . The two graphs correspond to  $\beta = 1$  and  $\beta = 1/16$ , respectively.

To see the SLAC/MIT phase transition we have to use another strategy. We use the rescaling adapted to the degenerate vacua situation  $a_n = n^{4/3}a_1$ ,  $b_n = n^{4/3}b_1$  and we take the potential to be

$$V(\chi) = \left(\chi^2 + \frac{1}{\sigma}\right)(\chi^2 - 1)^2 \quad (3.14)$$

so that a high value of  $\sigma$  corresponds to a small perturbation of the degenerate vacua potential (3.12). With this strategy it will be possible to detect the phase transition.

In Figure 11 we have plotted the tension for the degenerate vacua potential (3.12) and the perturbed degenerate vacua potential (3.14) with  $\sigma = 100$ . The tensions are the same up to  $n \sim 10^2$  and then the perturbed potential starts to deviate from the unperturbed one. Unfortunately the computation stops here and we cannot see that it enters in the MIT bag phase. Anyway the phase transition is clearly visible from the Figure.

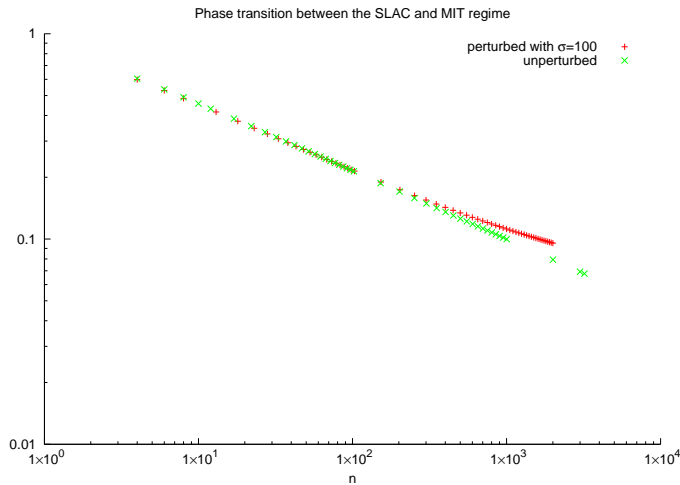


Figure 11: In this graph it is possible to see the phase transition between the SLAC regime and the MIT regime. The green points correspond to the degenerate vacua potential that is always in the SLAC regime. The red points correspond to the perturbed potential (3.14) with  $\sigma = 100$ . At  $n \sim 10^2$  there is a second order phase transition.

## 4 Conclusion and Further Developments

One of the most surprising aspects of the large  $n$  limit (2.9), is that the tension depends only on the value of the potential at zero  $V(0) = \varepsilon_0$ . If we have two different potentials with the same  $\varepsilon_0$ , the large  $n$  limit of the tension is the same.

Now we are going to argue something more. If we take two different potentials  $V_1(q)$  and  $V_2(q)$  with the same  $\varepsilon_0$  and the same  $q_0$ , not only the tensions are the same in the large  $n$  limit, but also are the profile functions.

The energy density derived from the Lagrangian (2.1) is the following

$$T_i[A, q] = 2\pi \int r dr \left[ \frac{1}{2e^2} \left( \frac{nA'}{r} \right)^2 + \frac{n^2}{r^2} (1 - A)^2 q^2 + q'^2 + V_i(q) \right], \quad (4.1)$$

where the index  $i = 1, 2$  refers to the potentials  $V_1$  and  $V_2$ , respectively. The energy density must be regarded as a functional: it takes the two profile function  $A(r)$  and  $q(r)$  and it gives out a number. The minimization of  $T_i[A, q]$  gives the profiles and the tension of the vortex. Now call  $A_1(r)$  and  $q_1(r)$  the profiles obtained by the minimization procedure for the potential  $V_1$ , and put them into the functional of the second potential. What we obtain is

$$T_2[A_1, q_1] = T_1[A_1, q_1] + 2\pi \int r dr [V_2(q_1) - V_1(q_1)] , \quad (4.2)$$

where we have simply added and subtracted  $V_1$ . In the large  $n$  limit the profile  $q_1(r)$  becomes a step function and, since the two potentials have the same  $\varepsilon_0$  and  $q_0$ , the extra piece  $2\pi \int r dr [V_2(q_1) - V_1(q_1)]$  vanishes. This means that the functions  $A_1(r)$  and  $q_1(r)$ , being the minima of the functional  $T_1$ , become also approximately the minima of the functional  $T_2$ .

*If the potential  $V_1(q)$  and  $V_2(q)$  have the same  $\varepsilon_0$  and the same  $q_0$ , the profile functions converge in the large  $n$  limit*

$$\lim_{n \rightarrow \infty} \|q_1 - q_2\| = 0 , \quad \lim_{n \rightarrow \infty} \|A_1 - A_2\| = 0 , \quad (4.3)$$

where the distance between functions is measured with the  $L^2$  metric. If the conjecture

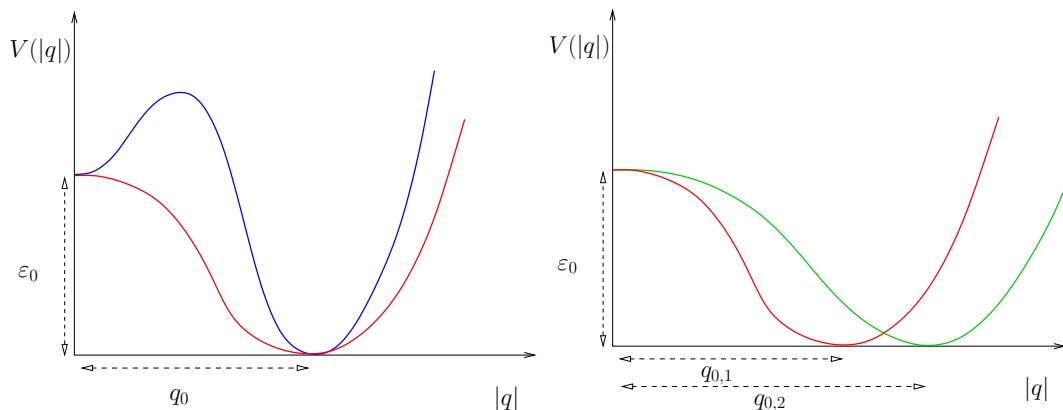


Figure 12: In the first sketch we have two different potentials with the same  $\varepsilon_0$  and the same  $q_0$ . In the second sketch we have two potentials with the same  $\varepsilon_0$  but different  $q_0$ .

is true we have also the following result. If the ratio between the zero energy density  $\varepsilon_0$  and the vev  $q_0$  is the same of the BPS potential, that is  $\varepsilon_0 = eq_0/2$ , whatever the shape of the potential, we recover supersymmetry in the large  $n$  limit. It is in fact

known that the Abelian-Higgs model with the BPS potential arise from the bosonic Lagrangian of SQED with zero mass and a Fayet-Ilyopoulos term [16]. In this case the “miracle” of the proportionality between the tension and the charge finds its explanation in the central charge of the supersymmetry algebra [15].<sup>3</sup>

In the present paper we have finally found a convincing proof that multi-vortices become bags in the large  $n$  limit. This fact is very general and applies also in the multi-monopole case [14]. It will be interesting to see if the bag mechanism works also in more general theories that contain solitons: nonabelian vortices [18], semi-local strings [20], Chern-Simon theories [19] and noncommutative field theories [21].

## Acknowledgments

We thank Mads T. Frandsen, Chris Kouvaris, Konstantin Petrov, Thomas Rytto and Francesco Sannino for useful discussions. S.B. wants to thank especially Roberto Auzzi, Jarah Evslin, Kenichi Konishi, and Marco Matone for comments and discussions. The work of S.B. is supported by the Marie Curie Excellence Grant under contract MEXT-CT-2004-013510 and by the Danish Research Agency.

## References

- [1] S. Bolognesi, Nucl. Phys. B **730**, 127 (2005) [arXiv:hep-th/0507273].
- [2] S. Bolognesi, Nucl. Phys. B **730**, 150 (2005) [arXiv:hep-th/0507286].
- [3] G. H. Derrick, J. Math. Phys. **5** (1964) 1252.
- [4] V. L. Ginzburg and L. D. Landau, Zh. Eksp. Teor. Fiz. **20** (1950) 1064.
- [5] A. A. Abrikosov, Sov. Phys. JETP **5** (1957) 1174 [Zh. Eksp. Teor. Fiz. **32** (1957) 1442].
- [6] H. B. Nielsen and P. Olesen, Nucl. Phys. B **61**, 45 (1973).
- [7] H. J. de Vega and F. A. Schaposnik, Phys. Rev. D **14** (1976) 1100.

---

<sup>3</sup>Even if the context is different, we just mention that there is another hot line of research in which non-supersymmetric gauge theories have supersymmetry relics in the large  $N$  limit [17].

- [8] L. Jacobs and C. Rebbi, Phys. Rev. B **19** (1979) 4486.
- [9] A. Chodos, R. L. Jaffe, K. Johnson, C. B. Thorn and V. F. Weisskopf, Phys. Rev. D **9** (1974) 3471.  
K. Johnson and C. B. Thorn, Phys. Rev. D **13** (1976) 1934.
- [10] W. A. Bardeen, M. S. Chanowitz, S. D. Drell, M. Weinstein and T. M. Yan, Phys. Rev. D **11** (1975) 1094.
- [11] R. Friedberg and T. D. Lee, Phys. Rev. D **16** (1977) 1096.
- [12] E. B. Bogomolny, Sov. J. Nucl. Phys. **24** (1976) 449 [Yad. Fiz. **24** (1976) 861].
- [13] E. J. Weinberg, Phys. Rev. D **19** (1979) 3008.  
C. H. Taubes, Commun. Math. Phys. **72** (1980) 277.
- [14] S. Bolognesi, “Multi-monopoles, Magnetic Bags and the Monopole Cosmological Problem”, *to appear*.
- [15] E. Witten and D. I. Olive, Phys. Lett. B **78**, 97 (1978).
- [16] J. D. Edelstein, C. Nunez and F. Schaposnik, Phys. Lett. B **329** (1994) 39 [arXiv:hep-th/9311055].
- [17] A. Armoni, M. Shifman and G. Veneziano, arXiv:hep-th/0403071.
- [18] R. Auzzi, S. Bolognesi, J. Evslin, K. Konishi and A. Yung, Nucl. Phys. B **673** (2003) 187 [arXiv:hep-th/0307287].  
A. Hanany and D. Tong, JHEP **0307** (2003) 037 [arXiv:hep-th/0306150].
- [19] R. Jackiw and E. J. Weinberg, Phys. Rev. Lett. **64** (1990) 2234.  
H. J. de Vega and F. A. Schaposnik, Phys. Rev. Lett. **56** (1986) 2564.  
G. V. Dunne, arXiv:hep-th/9902115.
- [20] T. Vachaspati and A. Achucarro, Phys. Rev. D **44** (1991) 3067.  
M. Hindmarsh, Phys. Rev. Lett. **68** (1992) 1263.  
A. Achucarro and T. Vachaspati, Phys. Rept. **327** (2000) 347 [Phys. Rept. **327** (2000) 427] [arXiv:hep-ph/9904229].

- [21] D. J. Gross and N. A. Nekrasov, JHEP **0007** (2000) 034 [arXiv:hep-th/0005204].  
M. R. Douglas and N. A. Nekrasov, Rev. Mod. Phys. **73** (2001) 977 [arXiv:hep-th/0106048].
- [22] A. M. Jaffe and C. Taubes, “Vortices And Monopoles. Structure Of Static Gauge Theories”.